https://doi.org/10.5194/egusphere-2026-2465
Preprint. Discussion started: 13 May 2026

Subseasonal predictability of compound heat and drought events in Europe

Rachel W.-Y. Wu[1,2], Dominik Büeler[1,3,4], Maria Pyrina[1,4,5], Jonathan Day[6], Adel Imamovic[3], Vincent Humphrey[3], and Daniela I.V. Domeisen[7,1]

[1]Institute for Atmospheric and Climate Science, ETH Zürich, Zürich, Switzerland
[2]Department of Applied Physics and Applied Mathematics, Columbia University, New York, USA
[3]Federal Office of Meteorology and Climatology MeteoSwiss, Zürich, Switzerland
[4]Center for Climate Systems Modeling, C2SM, Zürich, Switzerland
[5]European Centre for Medium-Range Weather Forecasts, ECMWF, Bonn, Germany
[6]European Centre for Medium-Range Weather Forecasts, ECMWF, Reading, UK
[7]Faculty of Geosciences and Environment, University of Lausanne, Lausanne, Switzerland

Correspondence: Rachel W.-Y. Wu, rw3191@columbia.edu

Abstract. Compound heat and drought events have severe socio-economic impacts on human health, agriculture and electricity supply. While these compound extremes are projected to intensify under climate change, our understanding of their subseasonal predictability remains limited compared to that of individual heat or drought events. In this study, we evaluate the predictability of compound heat and drought events over Europe using the subseasonal prediction system of the European Centre for Medium-Range Weather Forecasts (ECMWF). We find that the physical coupling between heat and drought contributes up to 10% towards an increase in forecast skill when heat and drought co-occur, relative to a baseline that assumes independence between extremes. However, in regions where the physical coupling between heat and drought via land-surface interaction is misrepresented, compound skill can be lower than when drought are predicted in isolation. These findings highlight the critical role of accurately simulating land-surface feedbacks to improve the reliability of the subseasonal prediction for compound extremes.

1 Introduction

Compound heat and drought events have wide-ranging socio-economic impacts, spanning human health (Campbell et al., 2018; Ebi et al., 2021), agriculture (Hatfield and Prueger, 2015; Brás et al., 2021), and electricity supply (Hawker et al., 2024; Li et al., 2025). Socio-economic impacts of compound extreme events can be mitigated by implementing early preventive measures based on skillful forecasts (Vitart and Robertson, 2018; Pegion et al., 2019; Lala et al., 2022; Dunn-Sigouin et al., 2025). As compound events are projected to become more frequent in the future under climate change (Seneviratne et al., 2021; AghaKouchak et al., 2020; Böhnisch et al., 2025), accurately predicting such extremes has become even more crucial.

The co-occurrence of extremes can be coincidental. However, shared physical drivers and feedbacks can enhance the correlation and the likelihood of compound extremes (Seneviratne et al., 2012). A primary driver of heat and drought events is an anomalous atmospheric circulation. For instance in the extratropics, quasi-stationary high-pressure systems, i.e. atmospheric

https://doi.org/10.5194/egusphere-2026-2465
Preprint. Discussion started: 13 May 2026

blocking, can contribute to surface heat (e.g. Barriopedro et al., 2011), typically through a mix of warm air advection (Cassou et al., 2005), adiabatic heating due to subsidence (Kautz et al., 2022; Sousa et al., 2018), and diabatic heating due to enhanced surface sensible heat fluxes driven by increased incoming solar radiation (Röthlisberger and Papritz, 2023). Apart from causing heat, atmospheric blocking systems additionally result in a precipitation deficit due to the deflection of synoptic cyclonic systems around them, which can lead to meteorological drought (Hao et al., 2018; Dai, 2011).

The correlation between surface temperature and precipitation can be further modulated by land-atmosphere feedbacks (Miralles et al., 2014; Seneviratne et al., 2010). High surface temperatures can accelerate soil moisture depletion in regions where evapotranspiration is soil-moisture limited, thereby amplifying drought conditions (Teuling et al., 2013). Conversely, soil-moisture depletion can trigger additional surface heating by enhancing sensible heat flux and reducing latent cooling, creating a positive feedback loop that intensifies surface temperature (Fischer et al., 2007b; Miralles et al., 2014, 2019; Benson and Dirmeyer, 2021). In contrast, in energy-limited regions where soil-moisture is more abundant, land-atmosphere coupling can exert a negative feedback on surface temperature, such that the evaporation of soil moisture due to radiation can dampen surface warming through the release of latent heat (Schwingshackl et al., 2017; Seneviratne et al., 2010). Depending on the type of soil-moisture and evapotranspiration regimes, land-atmosphere coupling can reinforce or dampen surface temperature (Seneviratne et al., 2006; Whan et al., 2015) and subsequently lead to more or fewer co-occurring heat and drought extremes.

Subseasonal and seasonal models demonstrate promising skill in forecasting summer temperatures (Prodhomme et al., 2022; Domeisen et al., 2023; Pyrina and Domeisen, 2023; Büeler et al., 2026). Skill for temperature has been shown to be even higher for hot extremes than for average events (Wulff and Domeisen, 2019), as demonstrated by successful predictions of individual heat waves (Luo and Zhang, 2012; Domeisen et al., 2022). In contrast, precipitation is considered one of the least predictable variables in subseasonal models (Li and Robertson, 2015; Prein et al., 2022). However, it has been argued that this apparent lack of skill may partially result from a 'double penalty' effect, as precipitation fields have sharp spatial and temporal gradients, unlike smoother fields such as temperature (Roberts and Lean, 2008; Lledó et al., 2023). As such, precipitation verification may be more representative when data is aggregated temporally or spatially by considering neighbouring grid points (Mittermaier and Roberts, 2010; Skok and Roberts, 2016).

Although the combination of heat and drought events is one of the most commonly studied compound event (Ridder et al., 2020; Brett et al., 2025), less is known about the predictability of this type of compound extreme. On some occasions, the skill in the prediction of low precipitation extremes has been found to be related to the skill in predicting heat extremes (Slater et al., 2019). This correlation of skill can arise from erroneous coupling in the models, for instance, because models produce a stronger coupling of drought to sea surface temperatures than observations suggest (Kam et al., 2014). However, there are also occasions where the coupling of skill originates from physical processes, such as land-atmosphere coupling (Fischer et al., 2007a). Soil-moisture-atmosphere interactions have been suggested to be an important driver of the 2003 European heat wave (García-Herrera et al., 2010; Fischer et al., 2007b). Improved representation of precipitation anomalies and soil-moisture conditions has been shown to enhance the prediction of heat waves, both through a better representation of dry conditions and through improved maintenance of quasi-stationary atmospheric circulation anomalies (DeAngelis et al., 2020), as demonstrated for the predictions of the 2003 European heat wave (Weisheimer et al., 2011) and the 2010 Russian heat wave (Seo et al., 2019).

https://doi.org/10.5194/egusphere-2026-2465
Preprint. Discussion started: 13 May 2026

In this study, we systematically evaluate the subseasonal predictability of compound heat and drought events across Europe. First, we identify the regions with concurrent heat and drought conditions. We then assess the predicability of these compound extremes using the subseasonal hindcasts from the European Center for Medium Range Weather Forecast (ECMWF). Finally, we explore model biases in land–atmosphere coupling as a potential physical explanation for the observed predictive skill.

2 Data and methods

2.1 Subseasonal hindcasts

ECMWF's subseasonal-range hindcasts (Vitart et al., 2017) cycle CY47R3 for the boreal summer (JJA) over the period 2002-2021 are analyzed in this study. The hindcasts, originally downloaded as daily means, are aggregated into monthly means by averaging the first four weeks following initialization (weeks 1-4). The hindcast climatology is computed for each initialization date using a centered 30-day approach, which takes the average of the hindcasts initialized within 15 calendar days before and after a given initialization date across the 20-year hindcast period. These climatologies are then subtracted from the aggregated values to obtain anomalies.

The choice of 1-month aggregation is motivated by the increased skill and practical utility of subseasonal forecasts at lead times beyond two weeks. Specifically, monthly aggregated anomalies have been demonstrated to be more skillfully predicted for European surface temperature than non-aggregated anomalies (Baker et al., 2023; Büeler et al., 2026). Furthermore, given that precipitation exhibits sharp temporal gradients (Lledó et al., 2023), temporal averaging enhances the utility of the forecasts. Such monthly aggregated quantities are used in operational monitoring platforms, such as, the Swiss national drought monitoring and early warning system at www.drought.admin.ch.

Since this model version is initialized twice per week, there are 26 initialization dates during each JJA season. Temporal aggregation is performed for each initialization date individually. Thus, these 1-month aggregation windows do not align with calendar months and exhibit substantial temporal overlaps between these windows. Given the temporal overlap, these 26 aggregated windows essentially function as a moving-window approach to identify periods of extreme conditions throughout the season. For further technical details regarding the computation of these aggregated anomalies and their corresponding climatologies, please refer to Büeler et al. (2026).

2.2 Observational datasets

The hindcasts are verified against ERA5 reanalysis (Hersbach et al., 2020), with ERA5 anomalies aggregated using the same temporal window as the hindcasts (as described in Section 2.1). These 1-month aggregated windows are computed relative to the hindcast start dates.

To evaluate soil-moisture-atmosphere coupling (Section 3.3), we follow the approach of Day et al. (2025) by using multiple observational datasets to evaluate land-atmosphere coupling. ERA5 exhibits known discontinuities in root-zone soil moisture (Muñoz-Sabater et al., 2021) and demonstrates lower performance in soil moisture compared to other satellite-derived or

https://doi.org/10.5194/egusphere-2026-2465
Preprint. Discussion started: 13 May 2026

model-based products (Beck et al., 2021). Thus, we use the Global Land Evaporation Amsterdam Model (GLEAM) version 3.7 (Miralles et al., 2011; Martens et al., 2017) for root-zone soil moisture (SM) and evapotranspiration (ET). For precipitation (P), we use the Global Precipitation Climatology Project (GPCP) version 2.3 (Adler et al., 2018), while for 2-m temperature (T_{2m}), ERA5 remains as the verification reference.

2.3 Heat, drought, and corresponding compound event definitions

Extreme events are identified at each grid point (i, j) for each 1-month aggregated window (n) using percentile-based thresholds. A heat event occurs when the 2-m temperature (T_{2m}) anomaly exceeds the 90th percentile of T_{2m} anomalies, while a drought event is defined as when total precipitation (P) anomaly falls below the 10th percentile of P anomalies. These percentiles are computed separately for the hindcasts and ERA5.

By using precipitation rather than soil moisture to define drought, we focus only on meteorological drought in this study. This approach ensures a clearer separation between the heat and drought definitions. Specifically, 2m-temperature and soil moisture are physically coupled through the land-surface energy balance, therefore defining drought via soil moisture would introduce a pre-existing dependency. In contrast, precipitation is an atmospheric variable. The use of precipitation to define meteorological drought keeps the heat and drought definitions more independent, which also allows for a more rigorous assessment of the hindcast's ability to predict compound events.

We define the frequency of heat (f_H), drought (f_D), and compound heat-drought (f_{CHD}) events as the fraction of initialization windows ($N = 26$) experiencing the extreme during each JJA season:

$$\mathrm{f_{i,j}} = \frac{\sum_{n=1}^{N} I_{i,j,n}}{N}; \qquad F_{i,j} = \frac{1}{20}\sum_{y=1}^{20} f_{i,j,y} \tag{1}$$

where $I_{i,j,n}$ is a binary indicator (1 for event occurrence, 0 otherwise). A compound event is defined when both heat and drought thresholds are met in the same 1-month aggregated window, with no lags considered. Finally, the annual frequencies are averaged over the 20-year study period to derive the climatological event frequency ($F_{i,j}$). The number of events defined per JJA are shown in Fig. C1-C3. The total number of events identified at each grid point across all 1-month windows (26 windows per JJA $\times$ 20 years = 520 windows) is shown in Fig. B1.

The 10th percentile threshold is roughly equivalent to a Standardized Precipitation Index (SPI) value of less than -1, a standard threshold that is commonly used in drought monitoring to identify events ranging from moderate to extreme drought (McKee et al., 1993). While a 10th percentile threshold is appropriate for identifying drought in predominantly non-arid regions of Europe, it is less suitable for semi-arid climates such as those in parts of the Iberian Peninsula (Morin et al., 2020; Middleton and Thomas, 1997). In these areas, the summer precipitation is climatologically so low that a 10th percentile threshold fails to distinguish extreme drought from typical dry conditions. Consequently, we restrict our analysis to grid points where the JJA precipitation (P) climatology exceeds 30 mm/month. This criterion effectively masks out large portions of the Iberian Peninsula (hatched in Fig. A1), regions typically classified as semi-arid (Morin et al., 2020).

https://doi.org/10.5194/egusphere-2026-2465
Preprint. Discussion started: 13 May 2026

2.4 Co-occurrence ratio (COR)

To quantify the degree to which compound events exceed their expected frequency under the assumption of independence, we employ the co-occurrence ratio (COR), following Messori et al. (2025). The COR is defined as:

$$\mathrm{COR} = 1 + \ln\left(\frac{F_{CHD}}{E_{CHD}}\right) \tag{2}$$

Here, E_{CHD} represents the expected climatological frequency of compound events, given by the product of the individual climatological occurrence of heat (F_H) and drought events (F_D). Given the 90th and 10th percentile thresholds used for heat and drought events, the expected occurrence of compound events is thus 1%. COR > 1 indicates that compound event occurrence is greater than expected by chance. COR = 1 indicates that the events are independent. COR < 1 indicates that events co-occur less frequently than expected under the assumption of independence.

2.5 Verification metrics

To evaluate the performance of the ensemble hindcasts, the fair Brier score (BS) by Ferro et al. (2008) is computed for each grid point by pooling all 1-month aggregated windows across the 20 years period:

$$BS = \frac{1}{K}\sum_{k=1}^{K}\left((p_k - o_k)^2 - \frac{m p_k (m - m p_k)}{m^2 (m-1)}\right) \tag{3}$$

where $K = 520$ is the total number of ensemble forecasts (26 forecasts per JJA $\times$ 20 years). Here, p_k is the forecasted probability, defined as the fraction of ensemble members (m=11) predicting an event, and o_k is the binary observation of event occurrence for the k-th window.

The BS is compared against the climatological Brier score (BS_{clim}) to evaluate the skilfulness of the forecasts. BS_{clim} is given by:

$$\mathrm{BS_{clim}} = \frac{1}{K}\sum_{k=1}^{K}(F_{i,j} - o_k)^2 \tag{4}$$

where $F_{i,j}$ is the climatological event occurrence as defined in Section 2.3. Finally, the Brier skill score (BSS) is defined as:

$$\mathrm{BSS} = 1 - \frac{\mathrm{BS}}{\mathrm{BS_{clim}}} \tag{5}$$

A BSS of 1 denotes a perfect forecast, while BSS = 0 indicates that the hindcast performance is equivalent to a climatological forecast. BSS > 0 indicates that the hindcast is more skilful than the climatology, whereas BSS < 0 indicates poorer skill.

To determine how much of the compound event skill stems from the model's ability to represent the physical coupling between heat and drought, we re-evaluate BSS_{CHD} under the assumption that these events are independent (BSS_{CHD_ind}).

https://doi.org/10.5194/egusphere-2026-2465
Preprint. Discussion started: 13 May 2026

In the standard BSS_{CHD}, the reference baseline is given by the climatological frequency of compound events (BS_{CHD_clim}). In the modified BSS_{CHD_ind}, BS_{CHD_clim} is replaced with a synthetic reference score (BS_{CHD_ind}). BS_{CHD_ind} is derived by assuming heat and drought occur independently. The expected frequency is calculated as the product of their individual climatological frequencies ($F_H \times F_D$), resulting in an expected occurrence of 1%.

By comparing BSS_{CHD} and BSS_{CHD_ind}, we can isolate the gain in skill attributed to the observed physical dependence between heat and drought. If BSS_{CHD_ind} is larger than BSS_{CHD}, it indicates that BS_{CHD_ind} is an easier reference to outperform than BS_{CHD_clim}. This suggests that the standard climatological reference (BS_{CHD_clim}), which inherently includes information regarding the physical coupling of heat and drought, in turn contributes to the overall predictive skill for compound events.

To aid the interpretation of the BSS, which evaluates probabilistic skill, we also calculate the False Alarm Ratio (FAR) and Hit Rate (HR), which measure the accuracy for binary categorical predictions. To transform the probabilistic ensemble into a categorical forecast, we classify an event as a 'hit' ('false') if at least 50% of the ensemble members (i.e. 6 out of 11 members) predicted an event that occurred (did not occur).

The FAR measures the proportion of forecasted events that did not occur (false positives) and is defined as:

$$\mathrm{FAR} = \frac{\mathrm{FP}}{\mathrm{TP} + \mathrm{FP}} \tag{6}$$

where TP represents true positives and FP represents false positives. The Hit Rate (HR) quantifies the fraction of observed events that were correctly predicted (true positives) and is given by:

$$\mathrm{HR} = \frac{\mathrm{TP}}{\mathrm{TP} + \mathrm{FN}} \tag{7}$$

where FN denotes false negatives. Both the FAR and the HR range from 0 to 1. Perfect predictive skill is characterized by $\mathrm{FAR} = 0$ (no false alarms) and $\mathrm{HR} = 1$ (all observed events successfully captured). As with the BSS, both metrics are calculated by pooling all one-month aggregated windows ($K = 520$).

2.6 Soil moisture-atmosphere coupling metrics

Following Dirmeyer (2011), Dirmeyer et al. (2014) and Day et al. (2025), we assess soil moisture-atmosphere coupling in the hindcasts by computing both the terrestrial and the atmospheric legs of coupling. The terrestrial leg measures the potential for soil moisture to influence the atmosphere via surface fluxes, while the atmospheric leg measures the influence of surface fluxes on the atmosphere state. A full land-atmosphere feedback exists only when both legs are active.

The strength of the terrestrial leg is defined as:

$$\mathrm{I}_{\mathrm{SM-ET}} = \sigma(\mathrm{ET})\rho(\mathrm{SM}, \mathrm{ET}) \tag{8}$$

https://doi.org/10.5194/egusphere-2026-2465
Preprint. Discussion started: 13 May 2026

where $\rho(SM, ET)$ is the correlation between soil moisture (SM) and evapotranspiration (ET), scaled by the standard deviation of ET ($\sigma(ET)$). Following the discussions in Seneviratne et al. (2010), a positive I_{SM-ET} denotes that soil-moisture constrains evapotranspiration (soil-moisture limited regime). And a near zero or negative I_{SM-ET} denotes that evapotranspiration is not limited by soil moisture but the available energy (energy limited regime).

The atmospheric leg is given by:

$$\mathrm{I_{SM-X}} = \sigma(X)\rho(\mathrm{SM}, \mathrm{ET})\rho(\mathrm{ET}, \mathrm{X}) \tag{9}$$

where X represents the atmospheric state, specifically T_{2m} or P in this study and $\sigma(X)$ is the standard deviation of X. An active land-atmosphere feedback is indicated by large magnitudes of I_{SM-X}, which result from high variance of X and strong correlations across both the terrestrial and atmospheric segments.

3 Results

3.1 Climatology and hotspots of compound heat and drought events over Europe

We first compute the frequency of occurrence of compound heat and drought events (F_{CHD}) in ERA5 reanalysis and subseasonal hindcasts (Fig. 1a-b). Across most of Europe, F_{CHD} exceeds 1%, which is the frequency expected under the assumption that heat (90th percentile) and drought (10th percentile) events are fully independent. The identified hotspots are qualitatively similar to those identified in Fig. 1b of Ridder et al. (2020). Compared to ERA5, the hindcasts underestimate F_{CHD} in regions where observed frequencies are relatively high, such as the British Isles and Central Europe, while overestimating frequencies across Eastern Europe (Fig. 1c).

To quantify the extent to which compound heat and drought events occur with a likelihood greater than expected under the assumption of independence, we compute the co-occurrence ratio (COR) for both ERA5 and the hindcasts (Fig. 1d, e). Consistent with Fig. 1a, b showing that F_{CHD} is greater than 1% in most regions, the COR exceeds 1 over most regions in Europe (Fig. 1d, e). The high COR across large parts of Europe reflects the fact that the co-occurrence of heat and drought is driven by common physical drivers, such as through large-scale atmospheric circulation (Dai, 2011; Hao et al., 2018) and land-atmosphere coupling (Seneviratne et al., 2010).

Spatially, the highest COR values are concentrated in Central and Southeastern Europe, and Russia, where compound events occur two to three times more often than expected under the assumption of independence. Regions where COR is relatively lower are parts of Western Europe (e.g. France) and Eastern Europe. While the hindcasts generally capture the spatial distribution of COR observed in ERA5, a notable difference is over Eastern Europe (Fig. 1f), where the hindcasts overestimate the frequency of compound events (Fig. 1c).

https://doi.org/10.5194/egusphere-2026-2465
Preprint. Discussion started: 13 May 2026

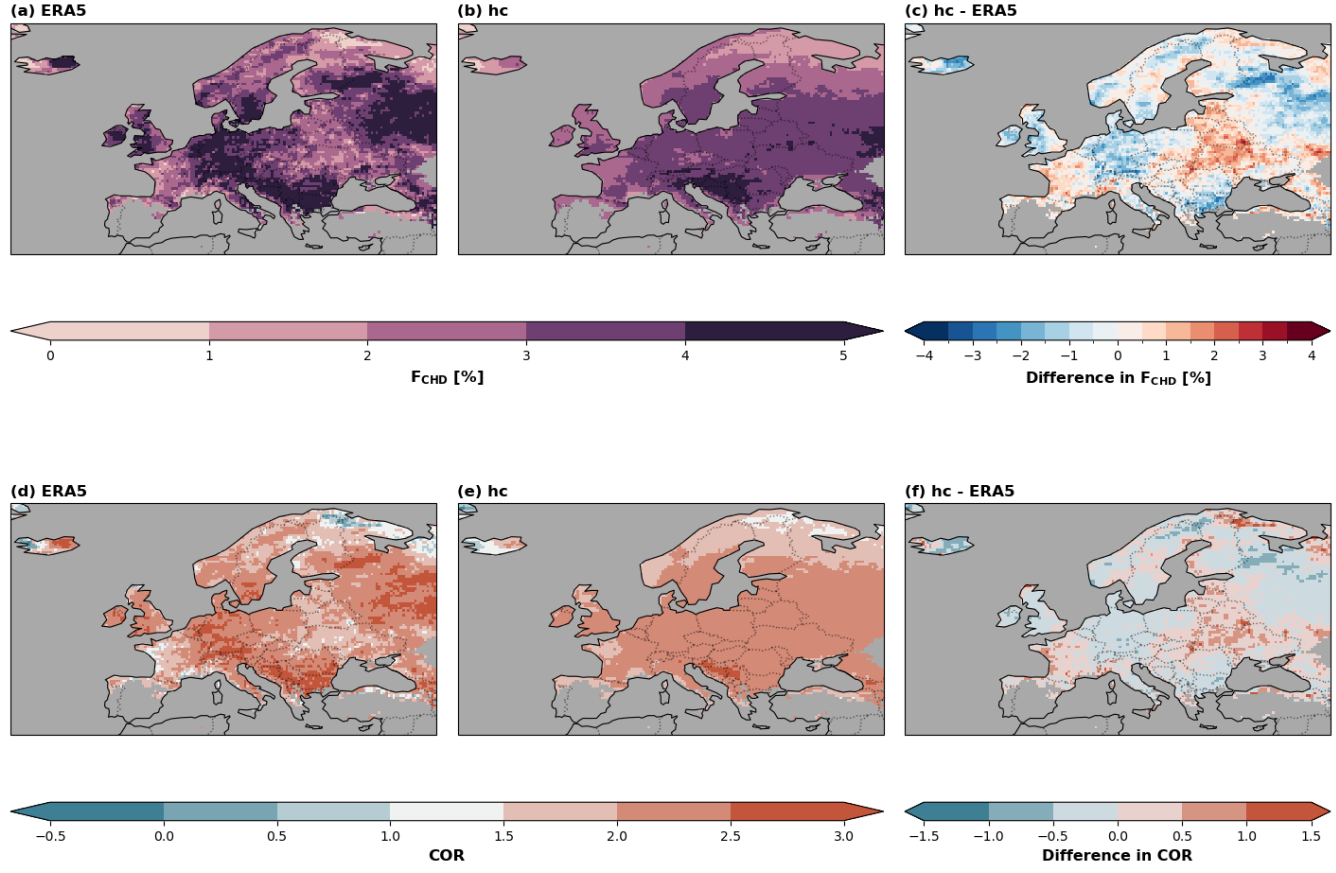

Figure 1. (a-c) Frequency of occurrence of compound heat and drought (CHD) events (F_{CHD}), expressed as the percentage of 1-month aggregated windows during JJA (26 windows per season) for (a) ERA5, (b) hindcasts (hc), and (c) the difference (hc - ERA5). (d-f) Co-occurrence ratio (COR) for ERA5, hc, and the difference (hc - ERA5). A COR > 1 indicates that the frequency of compound events exceeds what would be expected under the assumption of independence between hot and dry events. Only grid points where the JJA climatological mean monthly precipitation is greater than 30 mm/month are plotted.

3.2 Subseasonal predictability of heat, drought and corresponding compound events

We now investigate how well heat, drought, and compound heat and drought events are predicted in the subseasonal hindcasts (Fig. 2). Consistent with the known skilfulness of subseasonal hindcasts for temperature extremes (Domeisen et al., 2023; Prodhomme et al., 2022), the hindcasts exhibit highest BSS for heat events, compared to drought and compound events, with positive and statistically significant BSS across most parts of Europe (Fig. 2a).

Interestingly, the predictive skill for compound events (Fig. 2c) does not strictly follow the skill observed for drought alone (Fig. 2b). In regions such as Central Europe, Southeastern Europe, and the British Isles, the BSS for compound events is higher than for drought. This suggests that the higher predictability of heat extremes may enhance the overall skill of compound events in these regions. Conversely, compound event skill is lower than the skill of drought across large parts of of Scandinavia and

https://doi.org/10.5194/egusphere-2026-2465
Preprint. Discussion started: 13 May 2026

Eastern Europe (Fig. 2b,c). In Eastern Europe, this reduction in skill might stem from the overestimation of compound event occurrence and COR over this same region (Fig. 1c,f), suggesting that model biases in representing the joint occurrence of heat and drought can also degrade the predictive skill.

To isolate the gain in predictive skill derived from the physical coupling of heat and drought, we compare the standard BSS_{CHD} with a modified skill score BSS_{CHD_ind} (Fig. 3). For BSS_{CHD_ind}, the reference Brier Score is calculated under the assumption of independence between heat and drought occurrences (See Section 2.5). Across most of Europe, BSS_{CHD} is lower than BSS_{CHD_ind}, with the most pronounced differences (approximately -0.02 to -0.03) occurring over the compound event hotspots, such as Central and Southeastern Europe (Fig. 3c). The discrepancy between BSS_{CHD_ind} and BSS_{CHD} quantifies the skill contribution of the climatological coupling of heat and drought. Specifically, the lower BSS_{CHD} values indicate that the physical coupling present in the observed climatology provides a stricter and harder-to-beat baseline. The 0.03 reduction in skill when move from an independent to a physical coupled baseline suggests that approximately 10% of the apparent forecast skill in like Central Europe is inherently tied to the model's ability to represent this observed heat and drought coupling.

To further understand the regional differences in skill, we evaluate the Hit Rate (HR) and False Alarm Ratio (FAR) (Fig. 4). For heat events, the HR is the highest over Central Europe and Southwestern Scandinavia, while the lowest values are found over Eastern Europe and most of Northern Scandinavia (Fig. 4a). Dry events exhibit higher HR over Central Europe and Southeastern Europe (Fig. 4b). For compound events, HR is higher around Central and Eastern Europe (Fig. 4c).

In regions where the HR for heat is high, the FAR is correspondingly low, and vice versa (Fig. 4a, d). Comparing FAR for compound events (Fig. 4f) to drought (Fig. 4e), FAR for compound is lower than that for drought over Central Europe, British Isles and the Balkans. These regions coincide with regions where the compound BSS exceeds the drought BSS (Fig. 3b,c). Conversely, the compound FAR is substantially higher than the drought FAR over Eastern Europe (the Baltics, Belarus and Ukraine) and large parts of Scandinavia, the same regions where compound BSS is lower than drought BSS (Fig. 3b,c). The close agreement between the FAR and BSS patterns may suggest that the skill of compound events is constrained by false alarms in the model. Specifically, the model might benefit from high predictability of heat to improve compound event prediction over regions where temperature and drought coupling is correctly represented. However, in regions where both heat and drought FAR are high, for instance, over Eastern Europe, a misrepresented coupling might introduce more false alarms, further degrading the skill of compound events.

https://doi.org/10.5194/egusphere-2026-2465
Preprint. Discussion started: 13 May 2026

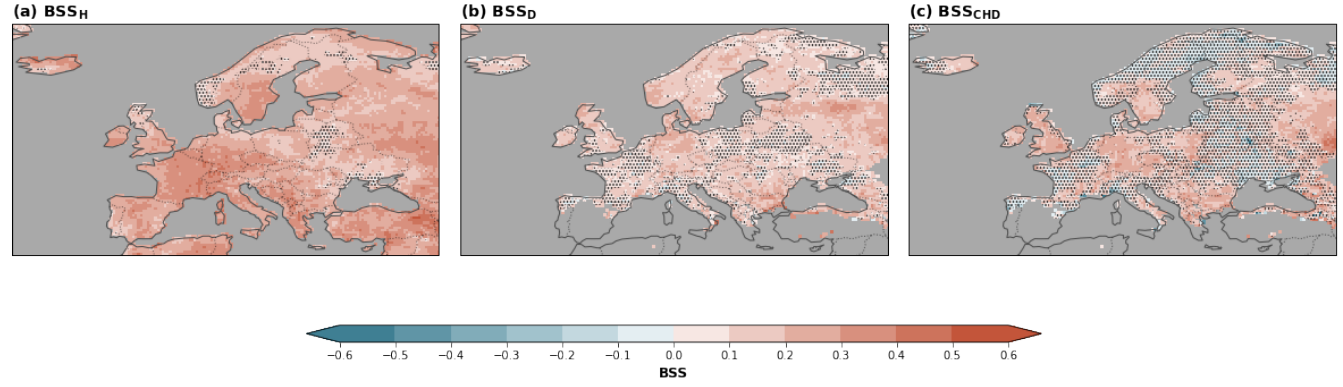

Figure 2. Brier skill score (BSS) of (a) hot (BSS_H), (b) drouught (BSS_D), and (c) compound heat and drought (BSS_{CHD}) extremes. The BSS is calculated using the ERA5 event climatology as the reference forecast, which is 10% by definition for hot and dry extremes respectively, and corresponds to values shown in Fig. 1a for compound extremes. Statistical significance is tested by bootstrapping with 1000 samples and regions that are non-statistically significant are indicated by stippling.

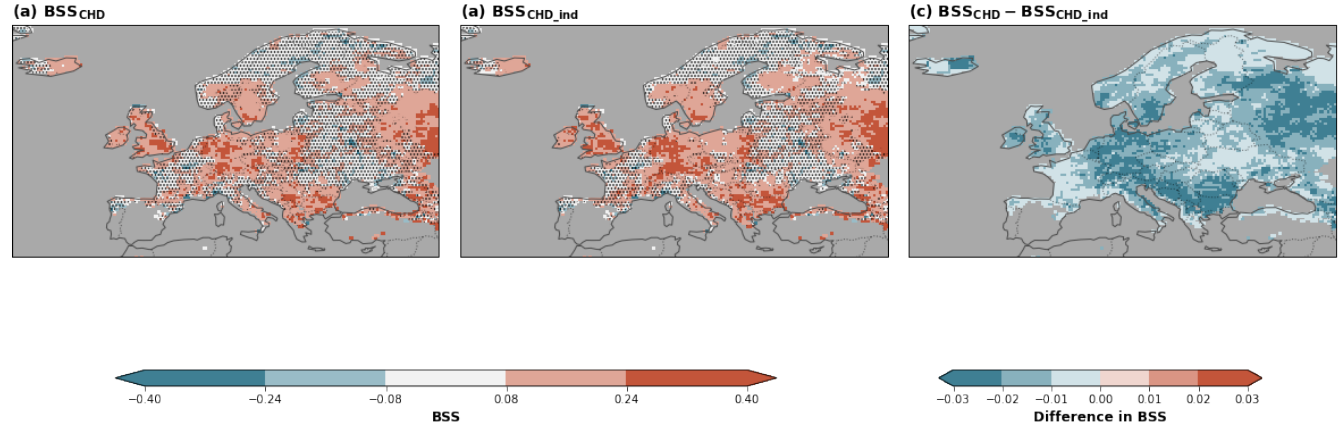

Figure 3. (a) BSS_{CHD} (re-plotted from Fig. 2c using a different color bar) and (b) the BSS for compound extremes calculated using the expected frequency under the assumption that the occurrence of hot and dry extremes is independent of each other (BSS_{CHD_ind}), which is 1% by definition. (c) The difference between BSS_{CHD} and BSS_{CHD_ind}. A negative difference indicates the skill "gain" resulting from the physical dependence between hot and dry extremes (i.e. the skill benefit when using the observed compound extremes climatology, rather than the independent 1% baseline, as the reference for the BSS calculation. Statistical significance is tested by bootstrapping with 1000 samples and regions that are non-statistically significant are indicated by stippling.)

https://doi.org/10.5194/egusphere-2026-2465
Preprint. Discussion started: 13 May 2026

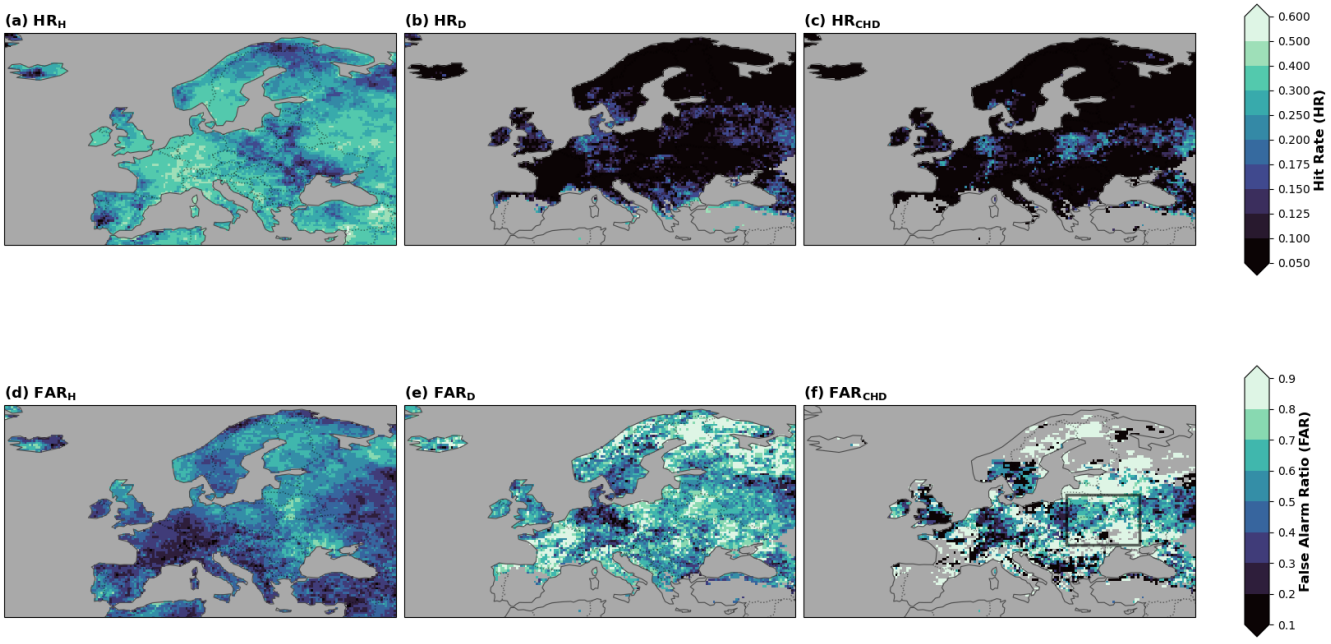

Figure 4. Hit rate (HR) and false alarm ratio (FAR) of (a) heat (H), (b) drought (D), and (c) compound heat and drought extremes (CHD). A "hit" in the hindcast is defined by a threshold where at least 50% of the ensemble members predict the event. The black box indicated in panel (f) defines the Eastern European study region (22°-35°E, 47°-56°N) that is used for the area-averaged scatter plot analysis in Fig. 6.

3.3 Role of land-atmosphere coupling biases in compound event false alarms

While anomalous atmospheric circulation is an important trigger for heat and drought events (e.g. Barriopedro et al., 2011; Hao et al., 2018), local land-atmosphere feedback plays a critical role in the amplification of such anomalies (e.g. Seneviratne et al., 2006). Day et al. (2025) identified biases in soil-moisture coupling within seasonal models which resulted in temperature forecast errors. Building on Day et al. (2025), we evaluate soil-moisture coupling biases in the sub-seasonal model and investigate how these biases might influence the predictive skill of compound heat and drought events.

Following Day et al. (2025), we first quantify soil moisture-atmosphere coupling in both observations and hindcasts by measuring the strength of the terrestrial and atmospheric legs (Fig. 5). The terrestrial leg, denoted by I_{SM-ET}, is positive over southern Europe in the observations, indicating that evapotranspiration is soil-moisture limited (Fig. 5a). In the hindcasts, I_{SM-ET} is stronger over Southeastern Europe, and these soil-moisture limited regions extend further into higher latitudes than observed (Fig. 5b). This results in a widespread positive bias, suggesting the hindcasts are too soil-moisture limited (Fig. 5c). These findings are consistent with the biases in seasonal forecasting systems identified by Day et al. (2025).

Regarding the atmospheric leg of land-atmosphere coupling, positive $I_{SM-T_{2m}}$ values are found over Eastern Europe, while negative values occur over Southwestern Scandinavia and Southern Europe (Fig. 5d). In the hindcasts, $I_{SM-T_{2m}}$ is less positive

https://doi.org/10.5194/egusphere-2026-2465
Preprint. Discussion started: 13 May 2026

over Eastern Europe and more negative and spatially extended over southern Europe (Fig. 5e). Consequently, the biases in $I_{SM-T_{2m}}$ are largely negative, except for Switzerland, Austria and Scandinavia, where positive biases emerge.

For the coupling with precipitation (I_{SM-P}), observations show scattered positive values across southeastern Europe and southwestern Scandinavia (Fig. 5g). In contrast, I_{SM-P} is more positive across most regions in the hindcasts, with the exception of the UK, Scandinavia and northern Russia (Fig. 5h). Overall, the hindcasts exhibit a positive I_{SM-P} bias (Fig. 5i).

Since hindcasts are more soil-moisture limited than observations (Fig. 5c), the negative $I_{SM-T_{2m}}$ bias and positive I_{SM-P} bias indicate an overly negative correlation between soil moisture with temperature, and an overly positive correlation between soil moisture with precipitation. Through these coupling pathways, these biases likely imply a misrepresented physical coupling between temperature and precipitation in the hindcasts.

To investigate how biases in soil-moisture coupling impact the forecast skill of compound events, we focus our analysis on Eastern Europe (indicated by the black box in Fig. 4f and Fig. 5c,f,i). Eastern Europe is selected because it exhibits the combination of negative $I_{SM-T_{2m}}$ and positive I_{SM-P} bias (Fig. 5f,i). Furthermore, this region is characterized by a high FAR (Fig. 4f), overestimation of compound heat and drought event frequency (Fig. 1c), and poor compound predictive skill (Fig. 2c).

As expected from the high I_{SM-ET} values in the hindcasts (Fig. 5b), a stronger correlation and more linear relation exists between soil moisture (SM) and evapotranspiration (ET) in the hindcasts compared to observations (Fig. 6d). Regarding the atmospheric leg, significant disparities emerge between the hindcasts and observations (Fig. 6b,c). While observations show a positive correlation between ET and temperature (T_{2m}) (Fig. 6b), the hindcasts fail to show a significant relationship. Conversely, the hindcasts exhibit a positive correlation between ET and precipitation (P) that is absent in the observations (Fig. 6c).

Since $I_{SM-T_{2m}}$ and I_{SM-P} are defined as the product of the correlation between SM and ET ($\rho(SM, ET)$) and the correlations between ET with T_{2m} and P respectively ($\rho(ET, T_{2m})$ and $\rho(ET, P)$) (see 2.6 in Methods), we can isolate the specific components of the coupling errors in the hindcasts. The weaker $\rho(ET, T_{2m})$ in the hindcasts (see R values in Fig. 6b) results in a weaker $I_{SM-T_{2m}}$ compared to observations (Fig. 5d,e), implying a weaker soil-moisture-temperature feedback (Fig. 5f). Conversely, the stronger $\rho(ET, P)$ (Fig. 6c) and $\rho(SM, ET)$ (Fig. 6d) in the hindcasts lead to a significantly more positive I_{SM-P} in hindcast (Fig. 5g,h), implying a stronger soil-moisture-precipitation feedback (Fig. 5i).

These biased soil-moisture feedbacks might thus have resulted in a more linear relationship between soil moisture with both T_{2m} and P in the hindcasts than in observations (Fig. 6e,f). By acting as a common driver, soil moisture induces a higher covariation between temperature and precipitation in the hindcasts than observations, as evidenced by the strengthened correlation between P and T_{2m} in the hindcasts (Fig. 6a). This stronger coupling between P and T_{2m} can explain the model's overestimation of compound events and the high false alarms over region (Fig. 1c, 4f), and thus the poorer predictive skill (Fig. 2c). When a drought is predicted, the hindcasts overconfidently expect a heat event to co-occur, and vice versa, due to the bias in the coupled soil-moisture feedback.

https://doi.org/10.5194/egusphere-2026-2465
Preprint. Discussion started: 13 May 2026

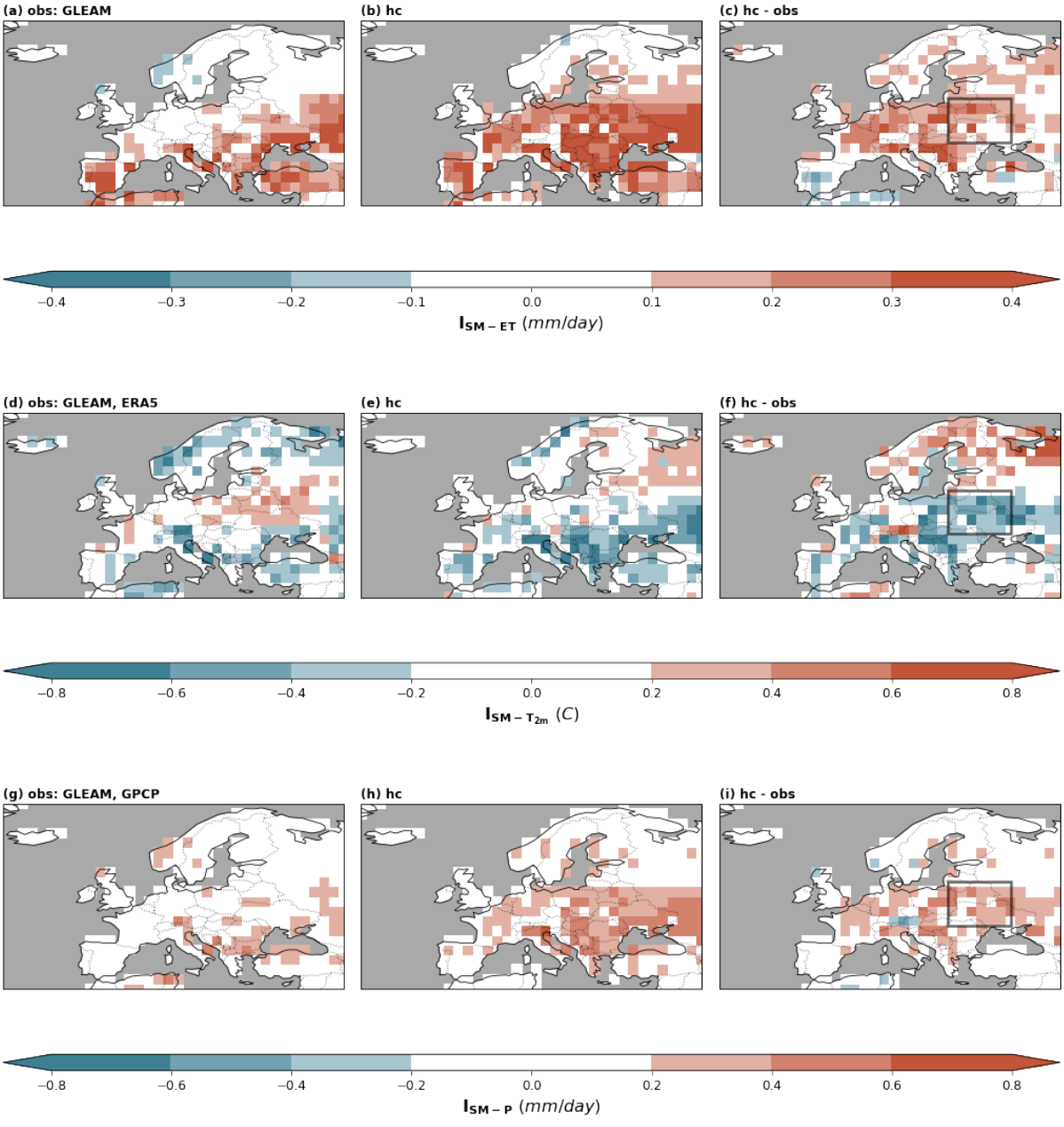

Figure 5. Land-atmosphere coupling metrics during JJA for observations, hindcasts and their differences. (a-c) The terrestrial leg (I_{SM-ET}), the atmospheric legs: (d-f) soil moisture-temperature coupling (I_{SM-T2m}), and (g-i) soil moisture-precipitation coupling ($I_{SM-totp}$). Columns represent (left) ERA5 observations, (center) hindcast ensemble means (hc), and (right) the model bias (hc − ERA5). To highlight regions with physically meaningful coupling strength, only values exceeding a threshold of ± 0.2 are shown. The black box indicated in panels (c), (f) and (i) defines the Eastern European study region (22°-35°E, 47°-56°N) that is used for the area-averaged scatter plot analysis in Fig. 6.

https://doi.org/10.5194/egusphere-2026-2465
Preprint. Discussion started: 13 May 2026

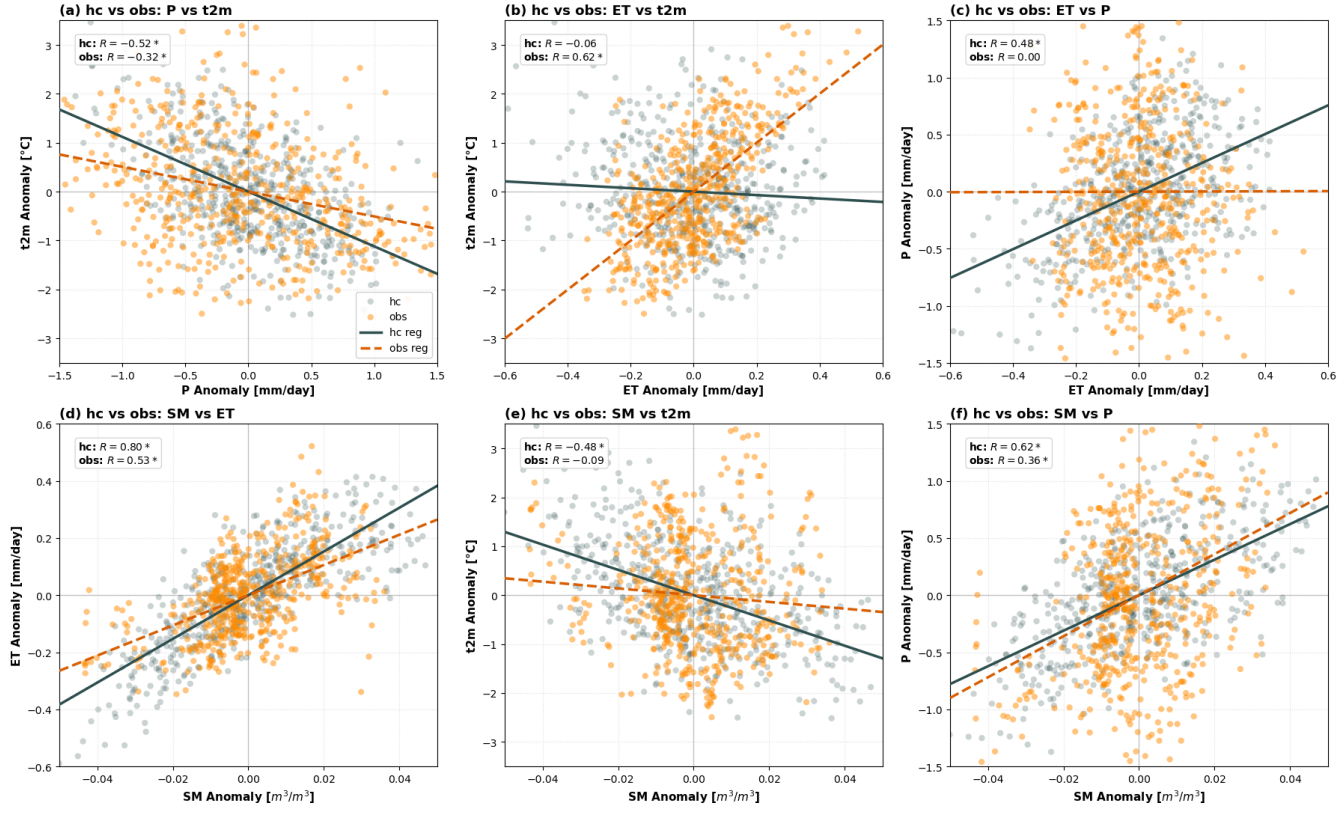

Figure 6. Relationships between land-atmosphere anomalies in observations (orange) and hindcast ensemble mean (bluegray). 1-month aggregated anomalies are shown for total precipitation (P), 2m-temperature (T_{2m}), evapotranspiration (ET), and top 1-meter soil moisture content (SM). Scatter plots illustrate the coupling between: (a) P vs. T_{2m}, (b) ET vs. T_{2m}, (c) ET vs. P, (d) SM vs. ET, (e) SM vs. T_{2m}, and (f) SM vs. P. All values represent the ensemble mean averaged over grid points within the Eastern European study region (22°-35°E, 47°-56°N, as indicated by the boxes in Fig. 5c,f,i). Regression lines are shown in solid line for hindcasts and dashed orange for observations; R denotes the Pearson correlation coefficient and stars indicate statistical significance ($p < 0.05$).

4 Conclusions

In this study, we investigate the predictability of monthly compound heat and drought events. Consistent with previous studies (e.g. Ridder et al., 2020), we identify Central, Southeastern and Northeastern Europe as regions with highest compound occurrence frequency over .

Using ECMWF subseasonal hindcasts, we evaluate the predictability of heat and drought events separately, and when they co-occur as compound events. We find that the hindcasts are generally more skillful in predicting heat events than drought or compound events. However, in several regions, namely Central Europe, Southeastern Europe and the British Isles, the skill for compound events exceeds that of drought events alone. By introducing a reference score that assumes independence between

https://doi.org/10.5194/egusphere-2026-2465
Preprint. Discussion started: 13 May 2026

temperature and precipitation, we quantify that the model's ability to represent the physical coupling of heat and drought contributes approximately 10% to the overall predictive skill of compound events in these regions.

Conversely, in some regions, the predictive skill for compound events is lower than for meteorological drought alone. We demonstrate that one of the reasons contributing to the poorer skill can emerge from a misrepresentationof the physical coupling between heat and drought. Specifically, we explore hindcast biases in land-atmosphere coupling as a potential source of erroneous temperature and precipitation coupling. Using Eastern Europe as an example, we show that a misrepresented land-atmosphere feedbacks, specifically a soil-moisture-tempereature feedback that is too weak and a soil-moisture-precipitation feedback that is too strong, lead to erroneous covariance between temperature and precipitation. This misrepresented coupling results in an overestimation of event frequency and false alarms, as the hindcasts predict the co-occurrence of heat and drought more frequently than observed.

In summary, the ECMWF subseasonal prediction system is skillful at capturing compound heat and drought events, particularly where the model correctly represents the underlying coupling. In these regions, the predictability of drought is effectively enhanced when it co-occurs with heat as compound events. Conversely, the reliability of heat and drought prediction is also impacted when the relationship between temperature and precipitation is misrepresented. While the origin of this erroneous coupling may lie in the model's land-atmosphere feedback mechanisms, it may also be inherited from reanalysis data, such as the known lower performance of soil moisture in ERA5 (Beck et al., 2021). While we have here limited the analysis of model biases to land-atmosphere coupling, other factors, such as the representation of quasi-stationary high pressure systems, remain subjects for future investigation.

By identifying regions of skillful compound predictions and providing physical justifications for model performance, this study enhances the confidence in forecasts, particularly in regions where the physical coupling is well-represented. As the co-occurrence of compound heat and drought extremes is projected to increase in a warming climate, addressing the model biases in these aforementioned physical mechanisms can improve the accuracy of subseasonal predictions, which may ultimately contribute to more accurate forecasts for stakeholders and the public to implement effective precautionary measures.

Data availability. ECMWF IFS hindcast data is available from the ECMWF public data archive (https://apps.ecmwf.int/archive- catalogue/). ERA5 data is available from the Copernicus Climate Data Store (https://cds.climate. copernicus.eu/datasets/reanalysis-era5-single-levels). The Python code used for analysis and visualization can be received from the authors upon request.

https://doi.org/10.5194/egusphere-2026-2465
Preprint. Discussion started: 13 May 2026

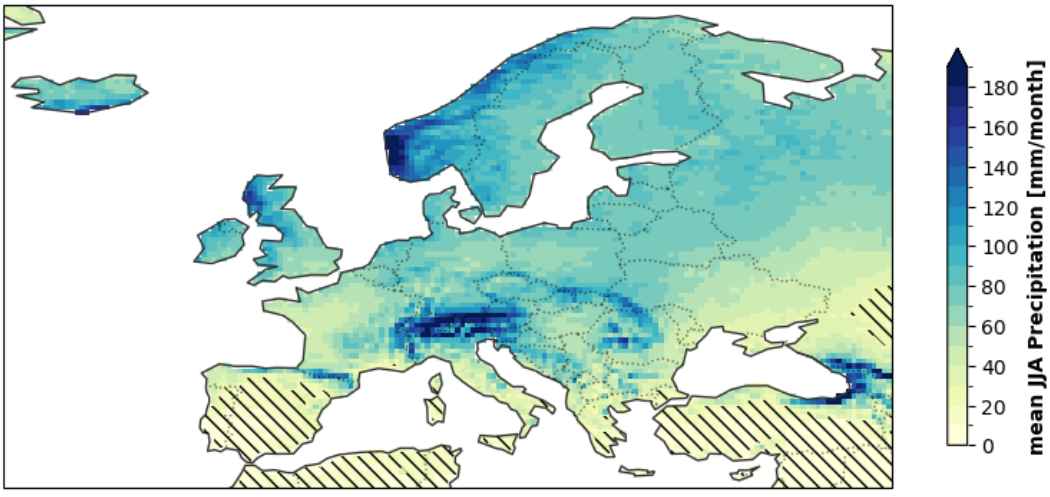

Figure A1. JJA climatology of 1-month aggregated total precipitation (P) in ERA5. Values represent the mean JJA precipitation for the period 2002–2021, corresponding to the period covered by the hindcasts. Grid points with a climatological mean below 30 mm/month are indicated by hatching and are excluded from the analysis in this study. Qualitatively, the hatched regions correspond well to the semi-arid regions as defined in, e.g., Morin et al. (2020).

Appendix A: Definition of semi-arid region

Appendix B: Total counts of identified heat, drought and compound events

Appendix C: Inter-annual counts of identified heat, drought and compound events

Appendix D: Representation of land-atmosphere coupling in hindcasts

Author contributions. RW, DB, MP, AI and DD designed the study. RW conducted the compound event analysis and hindcast verification, performed the data visualization and wrote the original manuscript draft. DB prepared and processed the monthly aggregated hindcasts and reanalysis data. JD performed the analysis of the soil moisture-atmosphere coupling metrics and the land-atmosphere anomaly scatter plots. AI and VH contributed to the conceptualization the study. DD acquired funding, conceptualized and supervised the study. All authors reviewed and revised the manuscript.

Competing interests. The contact author has declared that none of the authors has any competing interests.

https://doi.org/10.5194/egusphere-2026-2465
Preprint. Discussion started: 13 May 2026

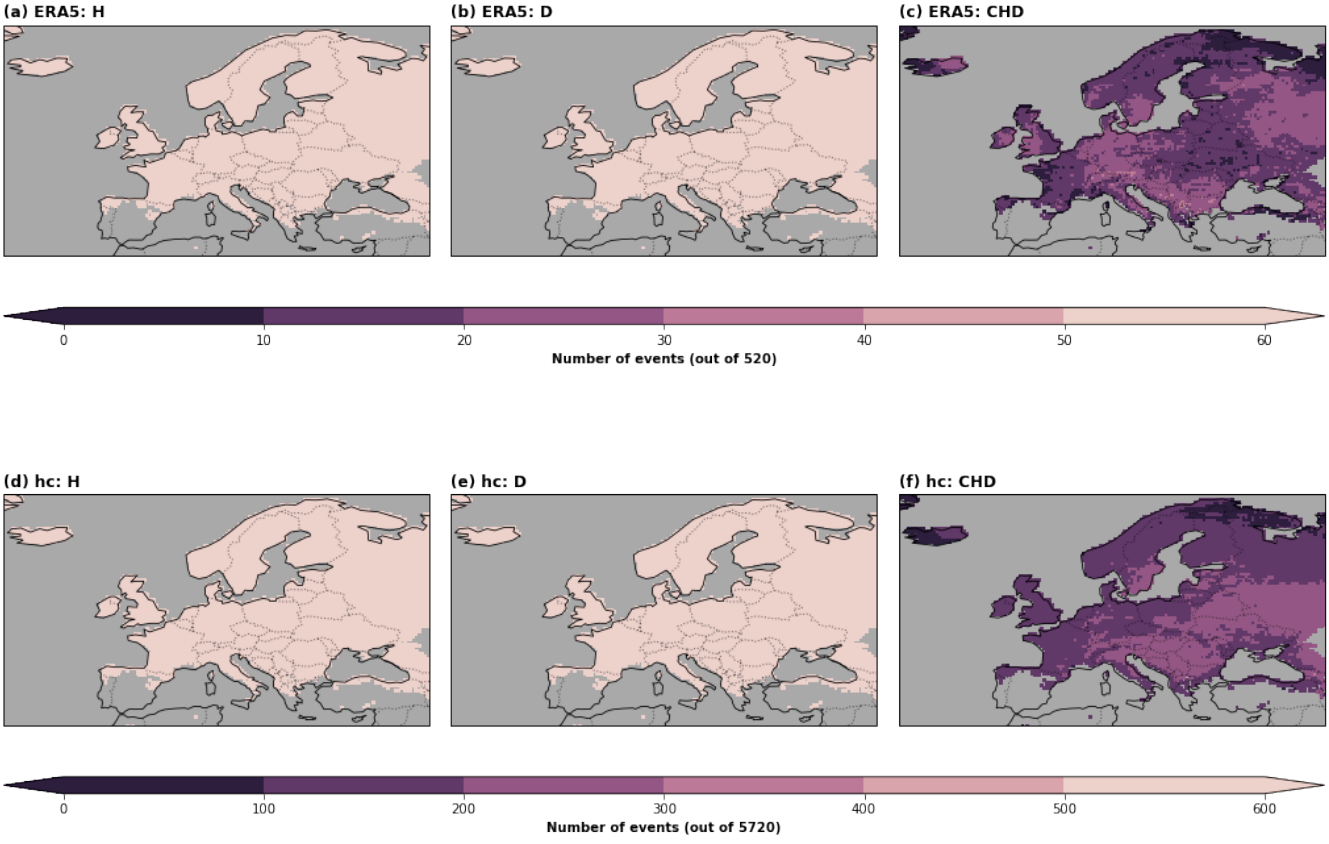

Figure B1. Total number of identified e xtreme e vents f or h eatwaves (H), d roughts (D), a nd c ompound h ot-dry (CHD) e xtremes. T op row displays ERA5 observations (520 total windows) and bottom row displays the hindcast ensemble mean (5720 total windows). By definition, H and D events represent the 90th and 10th percentile of the respective climatological distributions, resulting in 52 events per grid point in ERA5 and 572 events across all ensemble members in the hindcasts.

Acknowledgements. We acknowledge financial support from the Swiss drought program (https://www.meteoswiss.admin.ch/about-us/research-and-cooperation/projects/2024/drought-program.html). We acknowledge A. de Vries (Université de Lausanne) for downloading and providing ERA5 and ERA5-Land data. We would like to extend our gratitude to Christoph Spirig (MeteoSwiss) for fruitful discussions. The authors acknowledge the use of Gemini (Google) for the production of figures and grammatical refinement of the manuscript.

https://doi.org/10.5194/egusphere-2026-2465
Preprint. Discussion started: 13 May 2026

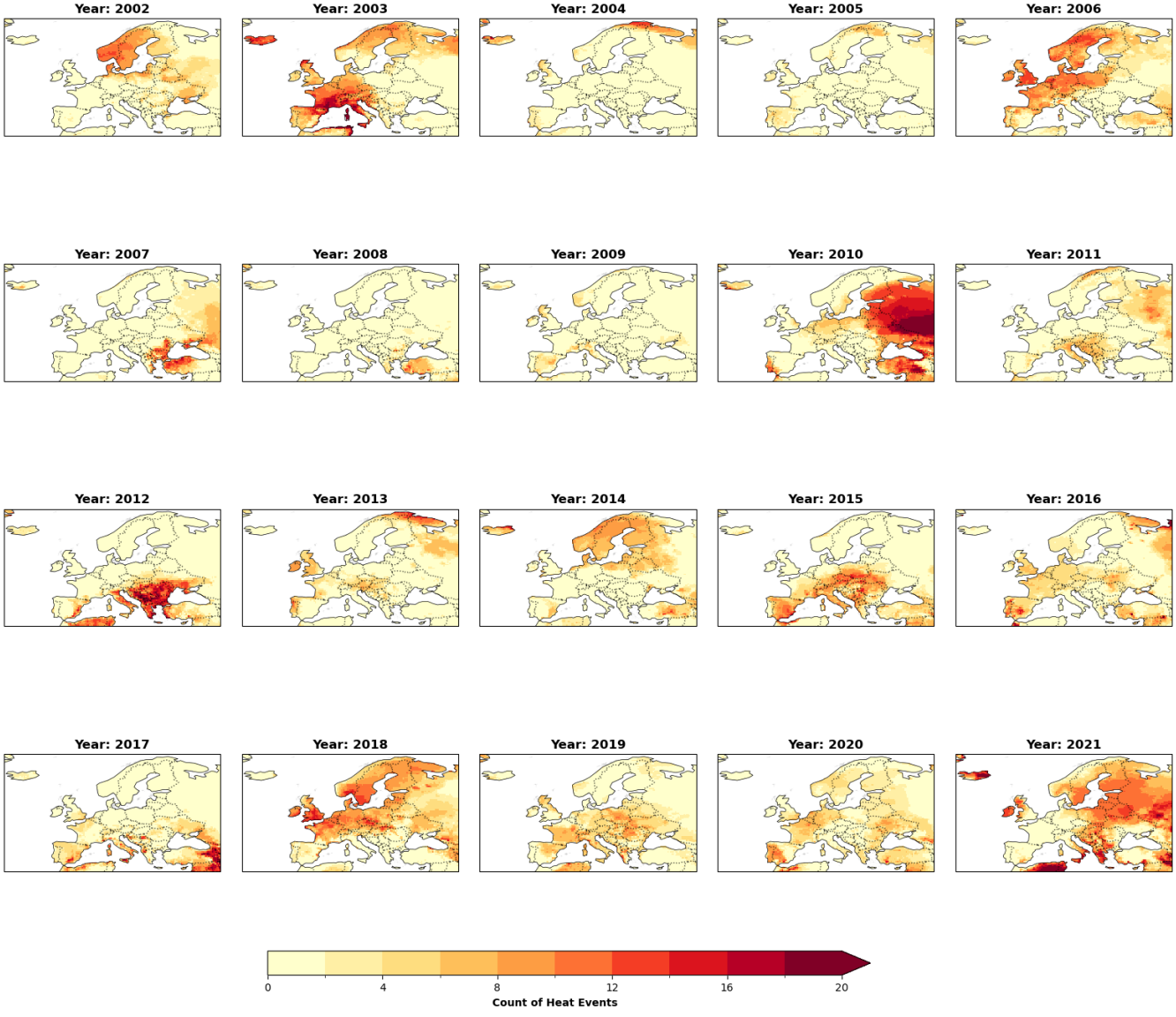

Figure C1. Inter-annual variability of hot extreme (H) counts in ERA5 for the JJA period (2002-2021). The counts represent the total number of windows identified as hot extremes each JJA, based on the 90th percentile threshold of 2m-temperature ($t2m$).

https://doi.org/10.5194/egusphere-2026-2465
Preprint. Discussion started: 13 May 2026

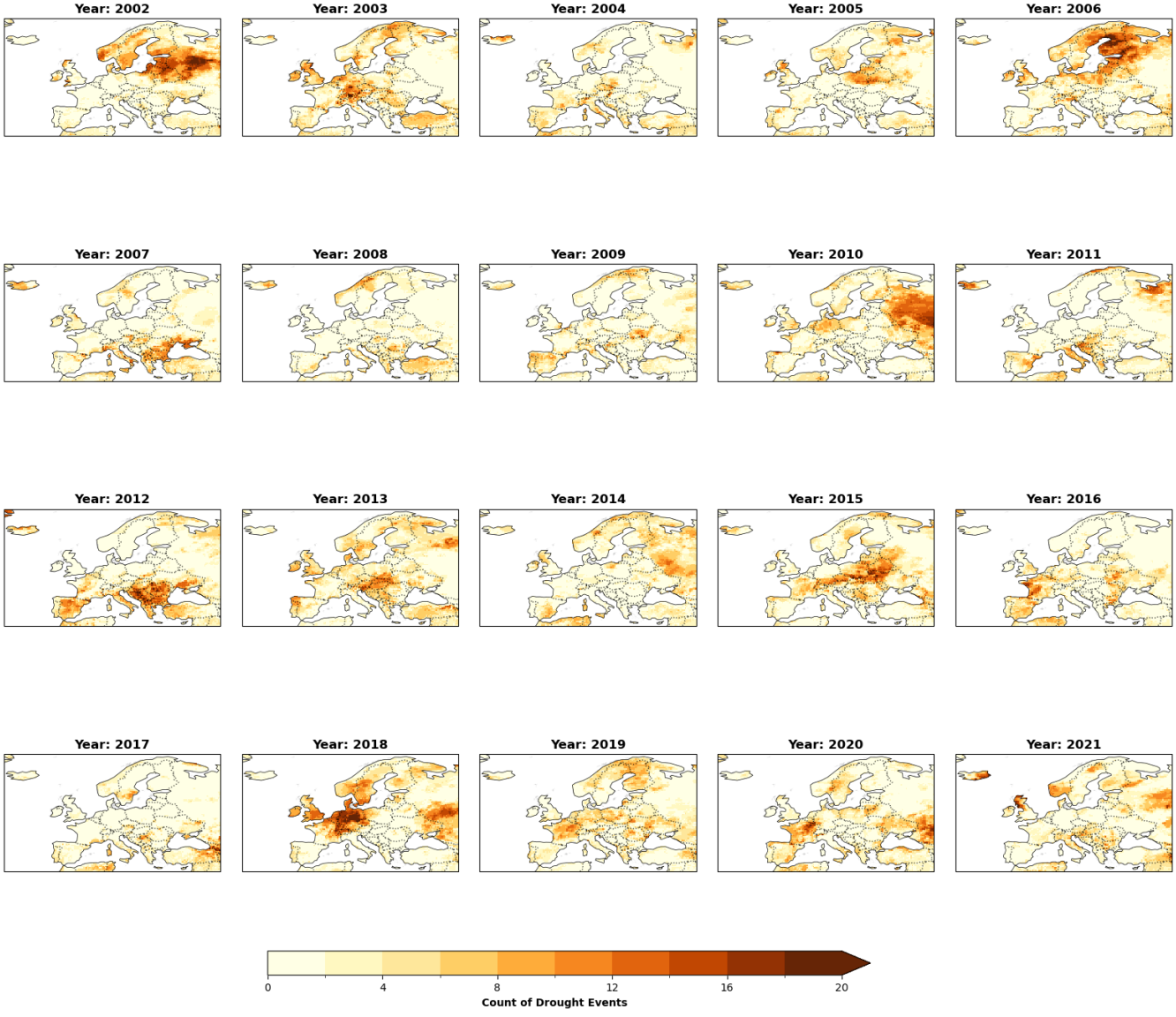

Figure C2. Inter-annual variability of dry extreme (D) counts in ERA5 for the JJA period (2002–2021). The counts represent the total number of windows identified as dry extremes each JJA, based on the 10th percentile threshold of total precipitation (*totp*).

https://doi.org/10.5194/egusphere-2026-2465
Preprint. Discussion started: 13 May 2026

Figure C3. Inter-annual variability of compound hot-dry (CHD) counts in ERA5 for the JJA period (2002–2021). The counts represent the total number of windows identified as compound extremes each JJA, defined by the simultaneous occurrence of a hot extreme ($>$ 90th percentile of $t2m$) and a dry extreme ($<$ 10th percentile of $totp$).

https://doi.org/10.5194/egusphere-2026-2465
Preprint. Discussion started: 13 May 2026

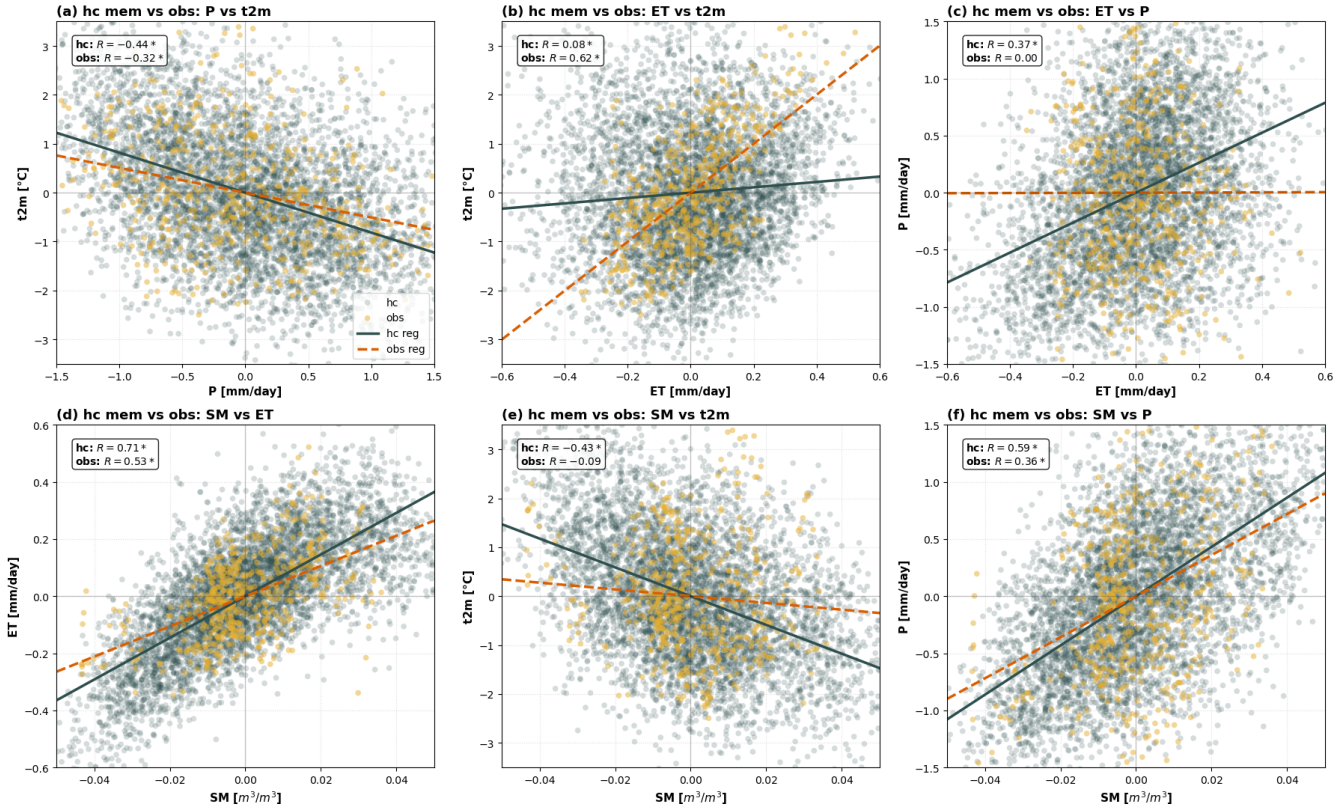

Figure D1. Same as Fig. 6, but hindcast ensemble members are plotted.

References

Adler, R. F., Sapiano, M. R. P., Huffman, G. J., Wang, J.-J., Gu, G., Bolvin, D., Chiu, L., Schneider, U., Becker, A., Nelkin, E., Xie, P., Ferraro, R., and Shin, D.-B.: The Global Precipitation Climatology Project (GPCP) Monthly Analysis (New Version 2.3) and a Review of 2017 Global Precipitation, Atmosphere, 9, 138, https://doi.org/10.3390/atmos9040138, 2018.

AghaKouchak, A., Chiang, F., Huning, L. S., Love, C. A., Mallakpour, I., Mazdiyasni, O., Moftakhari, H., Papalexiou, S. M., Ragno, E., and Sadegh, M.: Climate Extremes and Compound Hazards in a Warming World, Annu. Rev. Earth Planet. Sci., pp. 519–548, https://doi.org/10.1146/annurev-earth-071719-055228, 2020.

Baker, L., Charlton-Perez, A., and Mattu, K. L.: Skilful sub-seasonal forecasts of aggregated temperature over Europe, Meteorol. Appl., 30, e2169, https://doi.org/10.1002/met.2169, 2023.

Barriopedro, D., Fischer, E. M., Luterbacher, J., Trigo, R. M., and García-Herrera, R.: The Hot Summer of 2010: Redrawing the Temperature Record Map of Europe, Science, 332, 220–224, https://doi.org/10.1126/science.1201224, 2011.

Beck, H. E., Pan, M., Miralles, D. G., Reichle, R. H., Dorigo, W. A., Hahn, S., Sheffield, J., Karthikeyan, L., Balsamo, G., Parinussa, R. M., van Dijk, A. I. J. M., Du, J., Kimball, J. S., Vergopolan, N., and Wood, E. F.: Evaluation of 18 satellite- and model-based soil moisture products using in situ measurements from 826 sensors, Hydrol. Earth Syst. Sci., 25, 17–40, https://doi.org/10.5194/hess-25-17-2021, 2021.

https://doi.org/10.5194/egusphere-2026-2465
Preprint. Discussion started: 13 May 2026

Benson, D. O. and Dirmeyer, P. A.: Characterizing the Relationship between Temperature and Soil Moisture Extremes and Their Role in the Exacerbation of Heat Waves over the Contiguous United States, J. Clim., 34, 2175–2187, https://doi.org/10.1175/JCLI-D-20-0440.1, 2021.

Böhnisch, A., Felsche, E., Mittermeier, M., Poschlod, B., and Ludwig, R.: Future Patterns of Compound Dry and Hot Summers and Their Link to Soil Moisture Droughts in Europe, Earth's Future, 13, e2024EF004 916, https://doi.org/10.1029/2024EF004916, 2025.

Brás, T. A., Seixas, J., Carvalhais, N., and Jägermeyr, J.: Severity of drought and heatwave crop losses tripled over the last five decades in Europe, Environ. Res. Lett., 16, 065 012, https://doi.org/10.1088/1748-9326/abf004, 2021.

Brett, L., White, C. J., Domeisen, D. I., van den Hurk, B., Ward, P., and Zscheischler, J.: The growth in compound weather and climate event research in the decade since SREX, Natural Hazards and Earth System Sciences, 25, 2591–2611, 2025.

Büeler, D., Pyrina, M., Imamovic, A., Spirig, C., and Domeisen, D. I. V.: An opportunity index to anticipate when subseasonal predictions are useful, Q. J. R. Meteorolog. Soc., p. e70175, https://doi.org/10.1002/qj.70175, 2026.

Campbell, S., Remenyi, T. A., White, C. J., and Johnston, F. H.: Heatwave and health impact research: A global review, Health & Place, 53, 210–218, https://doi.org/10.1016/j.healthplace.2018.08.017, 2018.

Cassou, C., Terray, L., and Phillips, A. S.: Tropical Atlantic Influence on European Heat Waves, J. Clim., 18, 2805–2811, https://doi.org/10.1175/JCLI3506.1, 2005.

Dai, A.: Drought under global warming: a review, WIREs Clim. Change, 2, 45–65, https://doi.org/10.1002/wcc.81, 2011.

Day, J. J., Vitart, F., Stockdale, T., de Rosnay, P., Ardilouze, C., Peano, D., Sanna, A., Fröhlich, K., and Andrews, M.: Soil-moisture-atmosphere coupling hotspots and their representation in seasonal forecasts of boreal summer, Clim. Dyn., 63, 1–23, https://doi.org/10.1007/s00382-025-07753-1, 2025.

DeAngelis, A. M., Wang, H., Koster, R. D., Schubert, S. D., Chang, Y., and Marshak, J.: Prediction Skill of the 2012 U.S. Great Plains Flash Drought in Subseasonal Experiment (SubX) Models, J. Clim., 33, 6229–6253, https://doi.org/10.1175/JCLI-D-19-0863.1, 2020.

Dirmeyer, P. A.: The terrestrial segment of soil moisture–climate coupling, Geophys. Res. Lett., 38, https://doi.org/10.1029/2011GL048268, 2011.

Dirmeyer, P. A., Wang, Z., Mbuh, M. J., and Norton, H. E.: Intensified land surface control on boundary layer growth in a changing climate, Geophys. Res. Lett., 41, 1290–1294, https://doi.org/10.1002/2013GL058826, 2014.

Domeisen, D. I. V., White, C. J., Afargan-Gerstman, H., Muñoz, Á. G., Janiga, M. A., Vitart, F., Wulff, C. O., Antoine, S., Ardilouze, C., Batté, L., Bloomfield, H. C., Brayshaw, D. J., Camargo, S. J., Charlton-Pérez, A., Collins, D., Cowan, T., del Mar Chaves, M., Ferranti, L., Gómez, R., González, P. L. M., Romero, C. G., Infanti, J. M., Karozis, S., Kim, H., Kolstad, E. W., LaJoie, E., Lledó, L., Magnusson, L., Malguzzi, P., Manrique-Suñén, A., Mastrangelo, D., Materia, S., Medina, H., Palma, L., Pineda, L. E., Sfetsos, A., Son, S.-W., Soret, A., Strazzo, S., and Tian, D.: Advances in the Subseasonal Prediction of Extreme Events: Relevant Case Studies across the Globe, Bull. Am. Meteorol. Soc., 103, E1473–E1501, https://doi.org/10.1175/BAMS-D-20-0221.1, 2022.

Domeisen, D. I. V., Eltahir, E. A. B., Fischer, E. M., Knutti, R., Perkins-Kirkpatrick, S. E., Schär, C., Seneviratne, S. I., Weisheimer, A., and Wernli, H.: Prediction and projection of heatwaves, Nat. Rev. Earth Environ., 4, 36–50, https://doi.org/10.1038/s43017-022-00371-z, 2023.

Dunn-Sigouin, E., Kolstad, E. W., Ole Wulff, C., Parker, D. J., and Keane, R. J.: Balancing accuracy versus precision: Enhancing the usability of sub-seasonal forecasts, Clim. Serv., 39, 100 594, https://doi.org/10.1016/j.cliser.2025.100594, 2025.

https://doi.org/10.5194/egusphere-2026-2465
Preprint. Discussion started: 13 May 2026

Ebi, K. L., Capon, A., Berry, P., Broderick, C., de Dear, R., Havenith, G., Honda, Y., Kovats, R. S., Ma, W., Malik, A., Morris, N. B., Nybo, L., Seneviratne, S. I., Vanos, J., and Jay, O.: Hot weather and heat extremes: health risks, Lancet, 398, 698–708, https://doi.org/10.1016/S0140-6736(21)01208-3, 2021.

Ferro, C. A. T., Richardson, D. S., and Weigel, A. P.: On the effect of ensemble size on the discrete and continuous ranked probability scores, Meteorol. Appl., 15, 19–24, https://doi.org/10.1002/met.45, 2008.

Fischer, E. M., Seneviratne, S. I., Lüthi, D., and Schär, C.: Contribution of land-atmosphere coupling to recent European summer heat waves, Geophys. Res. Lett., 34, https://doi.org/10.1029/2006GL029068, 2007a.

Fischer, E. M., Seneviratne, S. I., Vidale, P. L., Lüthi, D., and Schär, C.: Soil Moisture–Atmosphere Interactions during the 2003 European Summer Heat Wave, J. Clim., 20, 5081–5099, https://doi.org/10.1175/JCLI4288.1, 2007b.

García-Herrera, R., Díaz, J., Trigo, R. M., Luterbacher, J., and Fischer, E. M.: A Review of the European Summer Heat Wave of 2003, Critical Reviews in Environmental Science and Technology, https://www.tandfonline.com/doi/full/10.1080/10643380802238137, 2010.

Hao, Z., Singh, V. P., and Xia, Y.: Seasonal Drought Prediction: Advances, Challenges, and Future Prospects, Rev. Geophys., 56, 108–141, https://doi.org/10.1002/2016RG000549, 2018.

Hatfield, J. L. and Prueger, J. H.: Temperature extremes: Effect on plant growth and development, Weather Clim. Extremes, 10, 4–10, https://doi.org/10.1016/j.wace.2015.08.001, 2015.

Hawker, G., Bell, K., Bialek, J., and MacIver, C.: Management of extreme weather impacts on electricity grids: an international review, Prog. Energy, 6, 032 005, https://doi.org/10.1088/2516-1083/ad3f6a, 2024.

Hersbach, H., Bell, B., Berrisford, P., Hirahara, S., Horányi, A., Muñoz-Sabater, J., Nicolas, J., Peubey, C., Radu, R., Schepers, D., Simmons, A., Soci, C., Abdalla, S., Abellan, X., Balsamo, G., Bechtold, P., Biavati, G., Bidlot, J., Bonavita, M., De Chiara, G., Dahlgren, P., Dee, D., Diamantakis, M., Dragani, R., Flemming, J., Forbes, R., Fuentes, M., Geer, A., Haimberger, L., Healy, S., Hogan, R. J., Hólm, E., Janisková, M., Keeley, S., Laloyaux, P., Lopez, P., Lupu, C., Radnoti, G., de Rosnay, P., Rozum, I., Vamborg, F., Villaume, S., and Thépaut, J.-N.: The ERA5 global reanalysis, Q. J. R. Meteorolog. Soc., 146, 1999–2049, https://doi.org/10.1002/qj.3803, 2020.

Kam, J., Sheffield, J., Yuan, X., and Wood, E. F.: Did a skillful prediction of sea surface temperatures help or hinder forecasting of the 2012 Midwestern US drought?, Environ. Res. Lett., 9, 034 005, https://doi.org/10.1088/1748-9326/9/3/034005, 2014.

Kautz, L.-A., Martius, O., Pfahl, S., Pinto, J. G., Ramos, A. M., Sousa, P. M., and Woollings, T.: Atmospheric blocking and weather extremes over the Euro-Atlantic sector – a review, Weather Clim. Dyn., 3, 305–336, https://doi.org/10.5194/wcd-3-305-2022, 2022.

Lala, J., Lee, D., Bazo, J., and Block, P.: Evaluating prospects for subseasonal-to-seasonal forecast-based anticipatory action from a global perspective, Weather Clim. Extremes, 38, 100 510, https://doi.org/10.1016/j.wace.2022.100510, 2022.

Li, J., Wu, J., Yang, Y., and Tang, R.: Economic consequences of compound drought-heatwave induced power deficits: evidence from Sichuan's 2022 power crisis, Sustainable Cities and Society, 130, 106 639, https://doi.org/10.1016/j.scs.2025.106639, 2025.

Li, S. and Robertson, A. W.: Evaluation of Submonthly Precipitation Forecast Skill from Global Ensemble Prediction Systems, Mon. Weather Rev., 143, 2871–2889, https://doi.org/10.1175/MWR-D-14-00277.1, 2015.

Lledó, L., Haiden, T., Schröttle, J., and Forbes, R.: Scale-dependent verification of precipitation and cloudiness at ECMWF, https://www.ecmwf.int/en/newsletter/174/earth-system-science/scale-dependent-verification-precipitation-and-cloudiness, [Online; accessed 2. Feb. 2026], 2023.

Luo, L. and Zhang, Y.: Did we see the 2011 summer heat wave coming?, Geophys. Res. Lett., 39, https://doi.org/10.1029/2012GL051383, 2012.

https://doi.org/10.5194/egusphere-2026-2465
Preprint. Discussion started: 13 May 2026

Martens, B., Miralles, D. G., Lievens, H., van der Schalie, R., de Jeu, R. A. M., Fernández-Prieto, D., Beck, H. E., Dorigo, W. A., and Verhoest, N. E. C.: GLEAM v3: satellite-based land evaporation and root-zone soil moisture, Geosci. Model Dev., 10, 1903–1925, https://doi.org/10.5194/gmd-10-1903-2017, 2017.

McKee, T. B., Doesken, N. J., and Kleist, J.: The relationship of drought frequency and duration to time scales, in: Proceedings of the 8th Conference on Applied Climatology, vol. 17, pp. 179–184, American Meteorological Society Boston, MA, 1993.

Messori, G., Muheki, D., Batibeniz, F., Bevacqua, E., Suarez-Gutierrez, L., and Thiery, W.: Global Mapping of Concurrent Hazards and Impacts Associated With Climate Extremes Under Climate Change, Earth's Future, 13, e2025EF006 325, https://doi.org/10.1029/2025EF006325, 2025.

Middleton, N. and Thomas, D. S. G.: World Atlas of Desertification, Arnold, London, 2nd edn., prepared for the United Nations Environment Programme, 1997.

Miralles, D. G., Holmes, T. R. H., De Jeu, R. A. M., Gash, J. H., Meesters, A. G. C. A., and Dolman, A. J.: Global land-surface evaporation estimated from satellite-based observations, Hydrol. Earth Syst. Sci., 15, 453–469, https://doi.org/10.5194/hess-15-453-2011, 2011.

Miralles, D. G., Teuling, A. J., van Heerwaarden, C. C., and Vilà-Guerau de Arellano, J.: Mega-heatwave temperatures due to combined soil desiccation and atmospheric heat accumulation, Nat. Geosci., 7, 345–349, https://doi.org/10.1038/ngeo2141, 2014.

Miralles, D. G., Gentine, P., Seneviratne, S. I., and Teuling, A. J.: Land–atmospheric feedbacks during droughts and heatwaves: state of the science and current challenges, Ann. N.Y. Acad. Sci., 1436, 19–35, https://doi.org/10.1111/nyas.13912, 2019.

Mittermaier, M. and Roberts, N.: Intercomparison of Spatial Forecast Verification Methods: Identifying Skillful Spatial Scales Using the Fractions Skill Score, Weather Forecasting, 25, 343–354, https://doi.org/10.1175/2009WAF2222260.1, 2010.

Morin, E., Marra, F., and Armon, M.: Dryland Precipitation Climatology from Satellite Observations, in: Satellite Precipitation Measurement, pp. 843–859, Springer, Cham, Switzerland, https://doi.org/10.1007/978-3-030-35798-6_19, 2020.

Muñoz-Sabater, J., Dutra, E., Agustí-Panareda, A., Albergel, C., Arduini, G., Balsamo, G., Boussetta, S., Choulga, M., Harrigan, S., Hersbach, H., Martens, B., Miralles, D. G., Piles, M., Rodríguez-Fernández, N. J., Zsoter, E., Buontempo, C., and Thépaut, J.-N.: ERA5-Land: a state-of-the-art global reanalysis dataset for land applications, Earth Syst. Sci. Data, 13, 4349–4383, https://doi.org/10.5194/essd-13-4349-2021, 2021.

Pegion, K., Kirtman, B. P., Becker, E., Collins, D. C., LaJoie, E., Burgman, R., Bell, R., DelSole, T., Min, D., Zhu, Y., Li, W., Sinsky, E., Guan, H., Gottschalck, J., Metzger, E. J., Barton, N. P., Achuthavarier, D., Marshak, J., Koster, R. D., Lin, H., Gagnon, N., Bell, M., Tippett, M. K., Robertson, A. W., Sun, S., Benjamin, S. G., Green, B. W., Bleck, R., and Kim, H.: The Subseasonal Experiment (SubX): A Multimodel Subseasonal Prediction Experiment, Bull. Am. Meteorol. Soc., 100, 2043–2060, https://doi.org/10.1175/BAMS-D-18-0270.1, 2019.

Prein, A. F., Towler, E., Ge, M., Llewellyn, D., Baker, S., Tighi, S., and Barrett, L.: Sub-Seasonal Predictability of North American Monsoon Precipitation, Geophys. Res. Lett., 49, e2021GL095 602, https://doi.org/10.1029/2021GL095602, 2022.

Prodhomme, C., Materia, S., Ardilouze, C., White, R. H., Batté, L., Guemas, V., Fragkoulidis, G., and García-Serrano, J.: Seasonal prediction of European summer heatwaves, Clim. Dyn., 58, 2149–2166, https://doi.org/10.1007/s00382-021-05828-3, 2022.

Pyrina, M. and Domeisen, D. I.: Subseasonal predictability of onset, duration, and intensity of European heat extremes, Quarterly Journal of the Royal Meteorological Society, 149, 84–101, 2023.

Ridder, N. N., Pitman, A. J., Westra, S., Ukkola, A., Do, H. X., Bador, M., Hirsch, A. L., Evans, J. P., Di Luca, A., and Zscheischler, J.: Global hotspots for the occurrence of compound events, Nat. Commun., 11, 5956, https://doi.org/10.1038/s41467-020-19639-3, 2020.

https://doi.org/10.5194/egusphere-2026-2465
Preprint. Discussion started: 13 May 2026

Roberts, N. M. and Lean, H. W.: Scale-Selective Verification of Rainfall Accumulations from High-Resolution Forecasts of Convective Events, Mon. Weather Rev., 136, 78–97, https://doi.org/10.1175/2007MWR2123.1, 2008.

Röthlisberger, M. and Papritz, L.: Quantifying the physical processes leading to atmospheric hot extremes at a global scale, Nat. Geosci., 16, 210–216, https://doi.org/10.1038/s41561-023-01126-1, 2023.

Schwingshackl, C., Hirschi, M., and Seneviratne, S. I.: Quantifying Spatiotemporal Variations of Soil Moisture Control on Surface Energy Balance and Near-Surface Air Temperature, J. Clim., 30, 7105–7124, https://doi.org/10.1175/JCLI-D-16-0727.1, 2017.

Seneviratne, S. I., Lüthi, D., Litschi, M., and Schär, C.: Land–atmosphere coupling and climate change in Europe, Nature, 443, 205–209, https://doi.org/10.1038/nature05095, 2006.

Seneviratne, S. I., Corti, T., Davin, E. L., Hirschi, M., Jaeger, E. B., Lehner, I., Orlowsky, B., and Teuling, A. J.: Investigating soil moisture–climate interactions in a changing climate: A review, Earth-Sci. Rev., 99, 125–161, https://doi.org/10.1016/j.earscirev.2010.02.004, 2010.

Seneviratne, S. I., Nicholls, N., Easterling, D., Goodess, C. M., Kanae, S., Kossin, J., Luo, Y., Marengo, J., McInnes, K., Rahimi, M., Reichstein, M., Sorteberg, A., Vera, C., and Zhang, X.: Changes in climate extremes and their impacts on the natural physical environment, in: Managing the Risks of Extreme Events and Disasters to Advance Climate Change Adaptation, edited by Field, C. B., Barros, V., Stocker, T. F., Qin, D., Dokken, D. J., Ebi, K. L., Mastrandrea, M. D., Mach, K. J., Plattner, G.-K., Allen, S. K., Tignor, M., and Midgley, P. M., pp. 109–230, Cambridge University Press, Cambridge, UK and New York, NY, USA, a Special Report of Working Groups I and II of the Intergovernmental Panel on Climate Change (IPCC), 2012.

Seneviratne, S. I., Zhang, X., Adnan, M., Badi, W., Dereczynski, C., Luca, A. D., Ghosh, S., Iskandar, I., Kossin, J., Lewis, S., Otto, F., Pinto, I., Satoh, M., Vicente-Serrano, S. M., Wehner, M., and Zhou, B.: Weather and Climate Extreme Events in a Changing Climate, in: Climate Change 2021: The Physical Science Basis. Contribution of Working Group I to the Sixth Assessment Report of the Intergovernmental Panel on Climate Change, edited by Masson-Delmotte, V., Zhai, P., Pirani, A., Connors, S. L., Péan, C., Berger, S., Caud, N., Chen, Y., Goldfarb, L., Gomis, M. I., Huang, M., Leitzell, K., Lonnoy, E., Matthews, J. B. R., Maycock, T. K., Waterfield, T., Yelekçi, O., Yu, R., and Zhou, B., pp. 1513–1766, Cambridge University Press, Cambridge, United Kingdom and New York, NY, USA, https://doi.org/10.1017/9781009157896.013, 2021.

Seo, E., Lee, M.-I., Jeong, J.-H., Koster, R. D., Schubert, S. D., Kim, H.-M., Kim, D., Kang, H.-S., Kim, H.-K., MacLachlan, C., and Scaife, A. A.: Impact of soil moisture initialization on boreal summer subseasonal forecasts: mid-latitude surface air temperature and heat wave events, Clim. Dyn., 52, 1695–1709, https://doi.org/10.1007/s00382-018-4221-4, 2019.

Skok, G. and Roberts, N.: Analysis of Fractions Skill Score properties for random precipitation fields and ECMWF forecasts, Q. J. R. Meteorolog. Soc., 142, 2599–2610, https://doi.org/10.1002/qj.2849, 2016.

Slater, L. J., Villarini, G., and Bradley, A. A.: Evaluation of the skill of North-American Multi-Model Ensemble (NMME) Global Climate Models in predicting average and extreme precipitation and temperature over the continental USA, Clim. Dyn., 53, 7381–7396, https://doi.org/10.1007/s00382-016-3286-1, 2019.

Sousa, P. M., Trigo, R. M., Barriopedro, D., Soares, P. M. M., and Santos, J. A.: European temperature responses to blocking and ridge regional patterns, Clim. Dyn., 50, 457–477, https://doi.org/10.1007/s00382-017-3620-2, 2018.

Teuling, A. J., Van Loon, A. F., Seneviratne, S. I., Lehner, I., Aubinet, M., Heinesch, B., Bernhofer, C., Grünwald, T., Prasse, H., and Spank, U.: Evapotranspiration amplifies European summer drought, Geophys. Res. Lett., 40, 2071–2075, https://doi.org/10.1002/grl.50495, 2013.

Vitart, F. and Robertson, A. W.: The sub-seasonal to seasonal prediction project (S2S) and the prediction of extreme events, npj Clim. Atmos. Sci., 1, 3, https://doi.org/10.1038/s41612-018-0013-0, 2018.

https://doi.org/10.5194/egusphere-2026-2465
Preprint. Discussion started: 13 May 2026

Vitart, F., Ardilouze, C., Bonet, A., Brookshaw, A., Chen, M., Codorean, C., Déqué, M., Ferranti, L., Fucile, E., Fuentes, M., Hendon, H., Hodgson, J., Kang, H.-S., Kumar, A., Lin, H., Liu, G., Liu, X., Malguzzi, P., Mallas, I., Manoussakis, M., Mastrangelo, D., MacLachlan, C., McLean, P., Minami, A., Mladek, R., Nakazawa, T., Najm, S., Nie, Y., Rixen, M., Robertson, A. W., Ruti, P., Sun, C., Takaya, Y., Tolstykh, M., Venuti, F., Waliser, D., Woolnough, S., Wu, T., Won, D.-J., Xiao, H., Zaripov, R., and Zhang, L.: The Subseasonal to Seasonal (S2S) Prediction Project Database, Bull. Am. Meteorol. Soc., 98, 163–173, https://doi.org/10.1175/BAMS-D-16-0017.1, 2017.

Weisheimer, A., Doblas-Reyes, F. J., Jung, T., and Palmer, T. N.: On the predictability of the extreme summer 2003 over Europe, Geophys. Res. Lett., 38, https://doi.org/10.1029/2010GL046455, 2011.

Whan, K., Zscheischler, J., Orth, R., Shongwe, M., Rahimi, M., Asare, E. O., and Seneviratne, S. I.: Impact of soil moisture on extreme maximum temperatures in Europe, Weather Clim. Extremes, 9, 57–67, https://doi.org/10.1016/j.wace.2015.05.001, 2015.

Wulff, C. O. and Domeisen, D. I. V.: Higher Subseasonal Predictability of Extreme Hot European Summer Temperatures as Compared to Average Summers, Geophys. Res. Lett., 46, 11 520–11 529, https://doi.org/10.1029/2019GL084314, 2019.